

# The GPIb $\alpha$ intracellular tail - role in transducing VWF- and collagen/GPVI-mediated signaling



Adela Constantinescu-Bercu,<sup>1</sup> Yuxiao A Wang,<sup>1</sup> Kevin J Woollard,<sup>2</sup> Pierre Mangin,<sup>3</sup> Karen Vanhoorelbeke,<sup>4</sup> James TB Crawley<sup>1</sup> and Isabelle I Salles-Crawley<sup>1</sup>

<sup>1</sup>Center for Hematology, Department of Immunology and Inflammation, Imperial College London, London, UK; <sup>2</sup>Center for Inflammatory Disease, Department of Immunology and Inflammation, Imperial College London, London, UK; <sup>3</sup>Université de Strasbourg, INSERM, EFS Grand-Est, BPPS UMR-S 1255, FMTS, Strasbourg, France and <sup>4</sup>Laboratory for Thrombosis Research, KU Leuven, Kortrijk, Belgium.

Haematologica 2022  
Volume 107(4):933-946

## ABSTRACT

The GPIb $\alpha$ -VWF A1 domain interaction is essential for platelet tethering under high shear. Synergy between GPIb $\alpha$  and GPVI signaling machineries has been suggested previously, however its molecular mechanism remains unclear. We generated a novel GPIb $\alpha$  transgenic mouse (*Gplb $\alpha$ <sup>Asig/Asig</sup>*) by CRISPR-Cas9 technology to delete the last 24 residues of the GPIb $\alpha$  intracellular tail that harbors the 14-3-3 and phosphoinositide-3 kinase binding sites. *Gplb $\alpha$ <sup>Asig/Asig</sup>* platelets bound von Willebrand factor (VWF) normally under flow. However, they formed fewer filopodia on VWF/biotin in the presence of a  $\alpha$ IIb $\beta$ 3 blocker, demonstrating that despite normal ligand binding, VWF-dependent signaling is diminished. Activation of *Gplb $\alpha$ <sup>Asig/Asig</sup>* platelets with ADP and thrombin was normal, but *Gplb $\alpha$ <sup>Asig/Asig</sup>* platelets stimulated with collagen-related-peptide (CRP) exhibited markedly decreased P-selectin exposure and  $\alpha$ IIb $\beta$ 3 activation, suggesting a role for the GPIb $\alpha$  intracellular tail in GPVI-mediated signaling. Consistent with this, while hemostasis was normal in *Gplb $\alpha$ <sup>Asig/Asig</sup>* mice, diminished tyrosine-phosphorylation, (particularly pSYK) was detected in CRP-stimulated *Gplb $\alpha$ <sup>Asig/Asig</sup>* platelets as well as reduced platelet spreading on CRP. Platelet responses to rhodocytin were also affected in *Gplb $\alpha$ <sup>Asig/Asig</sup>* platelets but to a lesser extent than those with CRP. *Gplb $\alpha$ <sup>Asig/Asig</sup>* platelets formed smaller aggregates than wild-type platelets on collagen-coated microchannels at low, medium and high shear. In response to both VWF and collagen binding, flow assays performed with plasma-free blood or in the presence of  $\alpha$ IIb $\beta$ 3- or GPVI-blockers suggested reduced  $\alpha$ IIb $\beta$ 3 activation contributes to the phenotype of the *Gplb $\alpha$ <sup>Asig/Asig</sup>* platelets. Together, these results reveal a new role for the intracellular tail of GPIb $\alpha$  in transducing both VWF-GPIb $\alpha$  and collagen-GPVI signaling events in platelets.

## Introduction

In order to fulfil their hemostatic function, platelets are recruited to sites of vessel damage by von Willebrand factor (VWF), which interacts with exposed collagen and, thereafter, to glycoprotein (GP) Ib $\alpha$  on the platelet via its A1 domain. VWF-mediated platelet tethering facilitates platelet capture.<sup>1</sup> Subsequent interaction of platelets with additional ligands (e.g.,  $\alpha$ IIb $\beta$ 3-fibrinogen, collagen-GPVI, collagen- $\alpha$ 2 $\beta$ 1) and changes in platelet phenotype are required to stabilize the platelet plug. Although the VWF-GPIb $\alpha$  interaction primarily facilitates platelet recruitment, it also transduces a signal that causes intraplatelet Ca<sup>2+</sup> release and activation of the platelet integrin,  $\alpha$ IIb $\beta$ 3.<sup>2,5</sup> These signaling events are highly dependent upon flow as shear forces induce unfolding of the GPIb $\alpha$  mechanosensitive juxtamembrane region that translates the mechanical signal into intracellular biochemical events.<sup>6,7</sup> Signaling is dependent upon the binding of adaptor and signaling molecules (e.g., Src kinases, Lyn and c-Src, 14-3-3 isoforms and phosphoinositide-3 kinase [PI3K]) that can associate with the GPIb $\alpha$  intracellular tail.<sup>8-12</sup> Downstream activation of phospholipase Cy2

## Correspondence:

ISABELLE I SALLES-CRAWLEY  
i.salles@imperial.ac.uk

Received: December 23, 2020.

Accepted: June 10, 2021.

Pre-published: June 17, 2021.

<https://doi.org/10.3324/haematol.2020.278242>

©2022 Ferrata Storti Foundation

Material published in *Haematologica* is covered by copyright. All rights are reserved to the Ferrata Storti Foundation. Use of published material is allowed under the following terms and conditions:

<https://creativecommons.org/licenses/by-nc/4.0/legalcode>.

Copies of published material are allowed for personal or internal use. Sharing published material for non-commercial purposes is subject to the following conditions:

<https://creativecommons.org/licenses/by-nc/4.0/legalcode>, sect. 3. Reproducing and sharing published material for commercial purposes is not allowed without permission in writing from the publisher.



(PLC $\gamma$ 2), PI3K-Akt, cGMP-PKG, mitogen activated kinase and LIM kinase 1 pathways have also been reported.<sup>13-19</sup> By comparison to other platelet agonists (e.g., collagen, thrombin, ADP, thromboxane A<sub>2</sub>), signaling through GPIIb $\alpha$  is considered weak. VWF-GPIIb $\alpha$  signaling, which we term platelet ‘priming’ rather than activation, does not induce appreciable degranulation.<sup>5</sup> Therefore, the contribution of platelet ‘priming’ to normal hemostasis remains unclear as the effects of the other platelet agonists have the potential to mask those of GPIIb $\alpha$ . However, in scenarios where other platelet agonists are either absent or in low abundance (e.g., platelet recruitment to endothelial or bacterial surfaces), the effects/importance of GPIIb $\alpha$  signaling may become more prominent.<sup>5</sup>

GPVI is a collagen/fibrin receptor on the platelet surface that non-covalently associates with Fc receptor  $\gamma$ -chain (FcR $\gamma$ ) and signals via immunoreceptor tyrosine-based activation motifs (ITAM).<sup>20-22</sup> Collagen binding to platelets induces clustering of GPVI, which results in the phosphorylation of FcR $\gamma$  by Src family kinases, Lyn and Fyn, that associate with the intracellular domain of GPVI.<sup>23,24</sup> This causes the recruitment and phosphorylation of Syk tyrosine kinase, and formation of a LAT-based signaling complex that can activate PLC $\gamma$ 2 and lead to release of intraplatelet Ca<sup>2+</sup> stores, activation of protein kinase (PK) C, and ultimately  $\alpha$ IIb $\beta$ 3 activation and both  $\alpha$ - and dense-granule release.<sup>21</sup>

Previous studies have suggested functional associations between GPIIb $\alpha$  and GPVI and/or its co-receptor FcR $\gamma$ .<sup>13,25,26</sup> For example, VWF-GPIIb $\alpha$ -mediated platelet responses are reportedly impaired in GPVI/FcR $\gamma$  deficiencies in both mice and humans.<sup>15,27</sup> There is also evidence that VWF can potentiate responses after collagen mediated responses in human platelets.<sup>28</sup> However, the molecular basis of GPIIb $\alpha$  and GPVI receptor crosstalk has not been elucidated. Using a novel GPIIb $\alpha$  transgenic mouse in which the last 24 amino acids (a.a.) of the GPIIb $\alpha$  intracellular tail were deleted, we demonstrate the importance of this region not only to VWF-dependent signaling in platelets, but also reveal a major contribution in augmenting GPVI-mediated platelet signaling.

## Methods

### Mice

All procedures were performed with the United Kingdom Home Office approval in accordance with the Animals (Scientific Procedures) Act of 1986. *Gplb $\alpha$ <sup>Asig/Asig</sup>* mice were generated in-house by the Medical Research Council transgenic group at Imperial College using CRISPR-Cas9 technology (Figure 1). Briefly, pronuclear injections (CBAB6F1) were performed with Cas9 mRNA (75 ng/ $\mu$ L), guide RNA (gRNA; 25-50 ng/ $\mu$ L) and single-strand oligo donor DNA (25-50 ng/ $\mu$ L). The donor DNA (GGTAAGGCC-TAATGGGCGAGTGGGGCCTCTGGTAGCAGGACGGC-GACCCTGAGCTCTGAGTCAGGGTCGTGGTCAGGACC-TATTGGGCACAGTGGGCATTA) had 50 bp homology arms at the 5' and 3' ends (Integrated DNA Technologies). Embryos were transferred to pseudo-pregnant CBAB6F1 female mice. Two founder mice originated from the same gRNA (CGACCCT-GACTCAGAGCTGAGGG) were bred with C57BL/6 mice. F1 *Gplb $\alpha$ <sup>Asig/+</sup>* mice were bred to obtain *Gplb $\alpha$ <sup>Asig/Asig</sup>* mice, and *Gplb $\alpha$ <sup>+/+</sup>* littermates were used as controls. Genotyping was performed by polymerase chain reaction (PCR) amplification of a *Gplb $\alpha$*  fragment (551 bp) using primers: AAGCACTCACACCACAAGCC

and AGTATGAATGAGCGGGAGCC and subsequent Sanger sequencing (Genewiz).

Experimental procedures were performed as previously described.<sup>29,30</sup> Additional details are included in the *Online Supplementary Appendix*.

## Results

### Generation of *Gplb $\alpha$ <sup>Asig/Asig</sup>* mice

Sequence identity between human and murine GPIIb $\alpha$  intracellular region is very high, supporting the contention that their functions are well conserved (Figure 1A). In order to evaluate the role of the GPIIb $\alpha$  intracellular tail upon both VWF- and collagen/GPVI-mediated signaling, we generated a novel transgenic mouse (*Gplb $\alpha$ <sup>Asig/Asig</sup>*) using CRISPR-Cas9 technology. We introduced a point mutation (Ser695Stop) that resulted in a premature stop codon that deletes the last 24 a.a. of the GPIIb $\alpha$  intracellular tail (a.a. 695-718) containing the entire 14-3-3 isoform and PI3K binding region,<sup>10,12</sup> but maintains the upstream filamin binding site in GPIIb $\alpha$  (residues 668-681 in murine GPIIb $\alpha$ )<sup>31</sup> (Figure 1A and B). Introduction of the mutation was confirmed by sequencing and by western blotting using an anti-GPIIb $\alpha$  antibody that recognizes the terminal region of the intracellular tail (Figure 1C to E). *Gplb $\alpha$ <sup>Asig/Asig</sup>* mice were viable and born with the expected Mendelian frequencies.

### *Gplb $\alpha$ <sup>Asig/Asig</sup>* mice platelet count, platelet size and hemostatic function

*Gplb $\alpha$ <sup>Asig/Asig</sup>* mice had mildly reduced (~20%) platelet counts and slightly larger platelet size (Figure 2A and B), but other hematological parameters were unaffected (*Online Supplementary Table S1*). This is in contrast to the severe thrombocytopenia and giant platelets observed in complete GPIIb $\alpha$  deficiency in mice or Bernard-Soulier patients.<sup>32,33</sup> Expression of the major platelet receptors, GPVI,  $\alpha$ IIb $\beta$ 3, GPIIb $\alpha$ , and the extracellular region of GPIIb $\alpha$  was unaltered on *Gplb $\alpha$ <sup>Asig/Asig</sup>* platelet surfaces (Figure 2C).

In order to assess hemostatic function in *Gplb $\alpha$ <sup>Asig/Asig</sup>* mice, we performed tail bleeding assays. Unlike *Vwf<sup>-/-</sup>* mice or mice lacking the extracellular domains of GPIIb $\alpha$ ,<sup>32,34,35</sup> *Gplb $\alpha$ <sup>Asig/Asig</sup>* mice displayed normal blood loss following tail transection (Figure 2D), suggesting that *Gplb $\alpha$ <sup>Asig/Asig</sup>* platelets can be recruited to sites of vessel damage similar to wild-type mice.

There was no difference between *Gplb $\alpha$ <sup>Asig/Asig</sup>* mice and wild-type littermates in a non-ablative laser-induced thrombus formation, as measured by the kinetics and extent, of both platelet accumulation and fibrin deposition (Figure 2E to G; *Online Supplementary Figure S1*; *Online Supplementary Video S1*).<sup>29,30,36</sup> These results support the contention that deletion of the GPIIb $\alpha$  does not appreciably influence either platelet recruitment or their ability to support thrombin generation. In this model, platelet accumulation requires both VWF and thrombin but has less dependency upon collagen exposure or GPVI signaling due to the non-ablative injury.<sup>37,38</sup>

### *Gplb $\alpha$ <sup>Asig/Asig</sup>* platelets bind von Willebrand factor (VWF) normally, but exhibit decreased VWF-mediated signaling

In order to specifically examine the effect of the GPIIb $\alpha$  intracellular tail truncation upon VWF-dependent platelet capture, we coated microchannels with murine VWF over

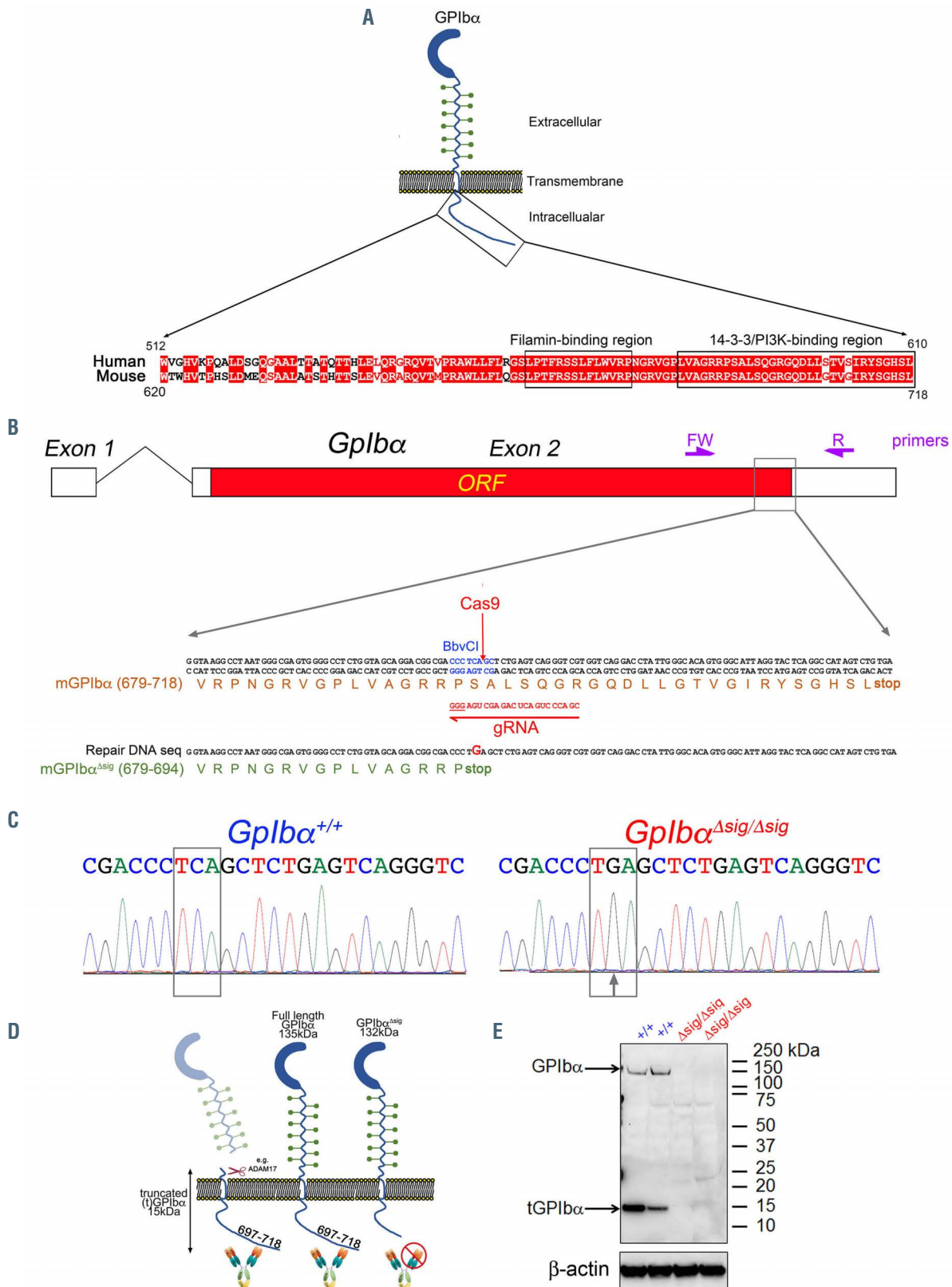


**Figure 1.** Generation and characterization of *Gplbα* $\Delta$ sig/ $\Delta$ sig mice. (A) Sequence alignment of the last 100 amino acids (a.a.) of human and mouse GPIb $\alpha$ . Sequence identities are highlighted in red. Filamin binding region: (a.a. 560-573) and (a.a. 668-681) for human and mouse GPIb $\alpha$ ; PI3K/14-3-3 binding region: (a.a. 580-610) and (a.a. 688-718) for human and mouse GPIb $\alpha$ . (B) Schematic representation of the *Gplbα* gene with CRISPR guide target site, gRNA sequence, BbvCI restriction enzyme site and Cas9 predicted cut site. Primers used to amplify the *Gplbα* allele from genomic DNA are indicated in purple. Design of the 101 bp single stranded DNA repair template with the point mutation to introduce a codon stop eliminating the BbvCI restriction enzyme site and removing the last 24 a.a. of GPIb $\alpha$  is also shown. The resulting truncated a.a. sequence from *Gplbα* $\Delta$ sig/ $\Delta$ sig mice is indicated in green. (C) Genomic DNA sequences from *Gplbα*<sup>+/+</sup> and *Gplbα* $\Delta$ sig/ $\Delta$ sig mice. Successful substitution is indicated with an arrow. (D) Diagram showing the binding of the anti-GPIb $\alpha$  tail Ab (Biorbyt; orb 215471). (E) Platelet lysates from *Gplbα*<sup>+/+</sup> and *Gplbα* $\Delta$ sig/ $\Delta$ sig mice were probed with the anti-GPIb $\alpha$  tail and  $\beta$ -actin antibodies. Absence of band in the GPIb $\alpha$  western-blot confirms the successful truncation of the GPIb $\alpha$  intracellular tail in *Gplbα* $\Delta$ sig/ $\Delta$ sig mice.

which we perfused plasma-free blood (to remove fibrinogen and outside-in activation  $\alpha\text{IIb}\beta\text{3}$ ) at  $1,000\text{s}^{-1}$ .  $Gplb\alpha^{\Delta\text{sig}/\Delta\text{sig}}$  platelets were recruited normally to murine VWF-coated surfaces with rolling velocities, surface coverage and platelet accumulation unaltered compared to  $Gplb\alpha^{+/+}$  platelets (Figure 3A to D; *Online Supplementary Video S2*).

In order to investigate the impact of the deletion of the last 24 a.a. of GPIb $\alpha$  on VWF signaling, we performed platelet spreading assays on murine VWF, which rely upon VWF-GPIb $\alpha$  signaling. On VWF alone, very few  $Gplb\alpha^{+/+}$  or

$Gplb\alpha^{\Delta\text{sig}/\Delta\text{sig}}$  platelets bound to VWF and only very few exhibited filopodia (Figure 3E and F). When these experiments were repeated in the presence of botrocetin (a snake venom that increases the affinity of VWF A1 domain for GPIb $\alpha$ )<sup>9,19</sup> a large proportion ( $90\pm 2.8\%$ ) of  $Gplb\alpha^{+/+}$  platelets underwent shape changes and developed filopodia (Figure 3E and G; *Online Supplementary Figure S2A and B*), a well-described consequence of VWF-GPIb $\alpha$  signaling.<sup>9,19</sup> This process was significantly diminished in  $Gplb\alpha^{\Delta\text{sig}/\Delta\text{sig}}$  platelets with only  $46\pm 2.6\%$  platelets exhibiting filopodia (Figure 3E

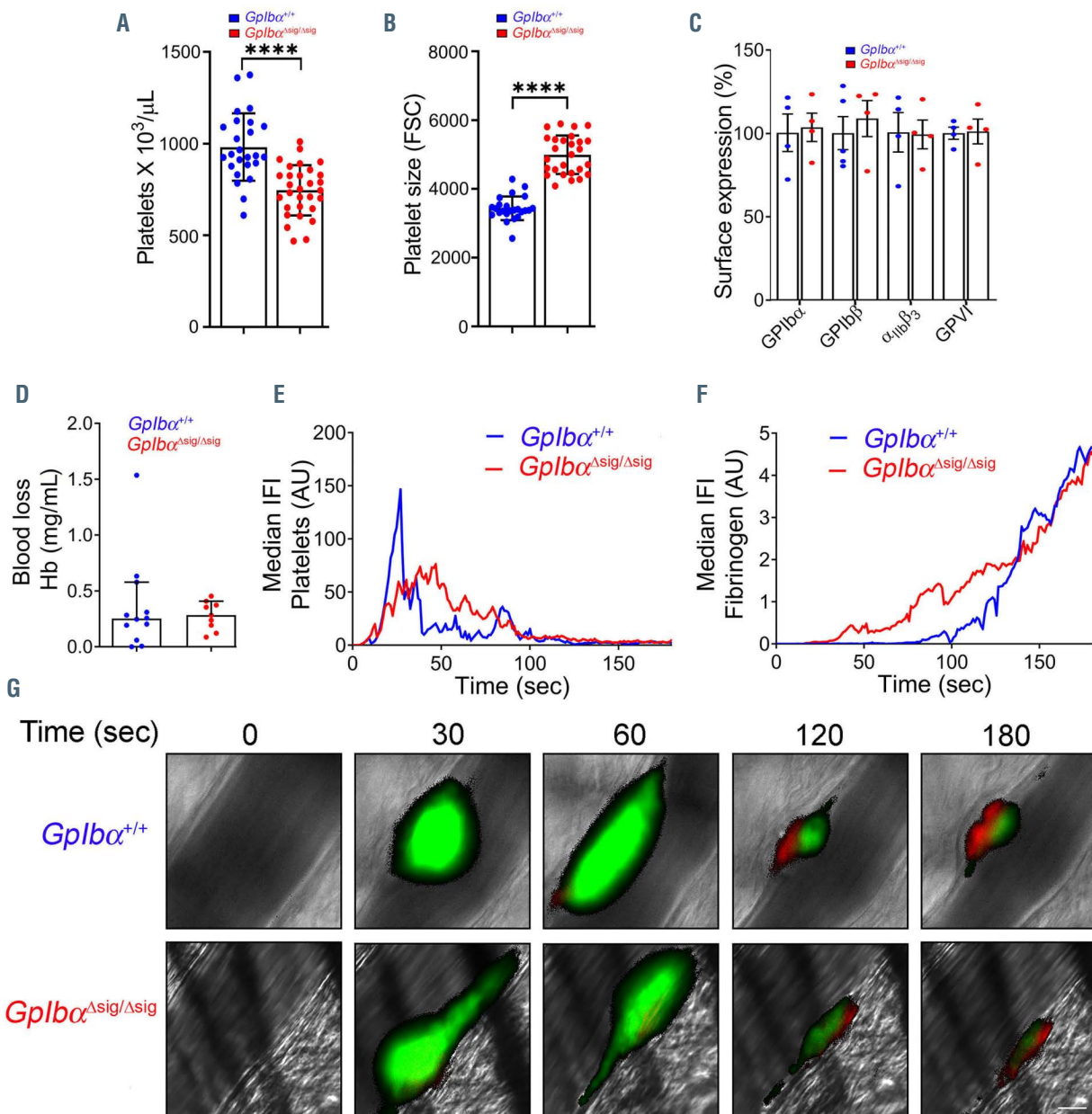


**Figure 2.**  $Gplb\alpha^{\Delta\text{sig}/\Delta\text{sig}}$  mice display normal bleeding loss and platelet and fibrin accumulation in the laser-induced thrombosis model. A) Platelet counts and (B) platelet size in  $Gplb\alpha^{+/+}$  ( $n=25$ ) and  $Gplb\alpha^{\Delta\text{sig}/\Delta\text{sig}}$  mice ( $n=30$ ) as determined by flow cytometry. (C) Surface expression of platelet receptors GPIb $\alpha$ , GPIIb/III $\alpha$  and GPVI in  $Gplb\alpha^{+/+}$  and  $Gplb\alpha^{\Delta\text{sig}/\Delta\text{sig}}$  mice ( $n=4$  for each genotype) determined by flow cytometry and expressed as % of control. (D) Bar graph analyzing blood loss after 10 minutes following tail transection in  $Gplb\alpha^{+/+}$  and  $Gplb\alpha^{\Delta\text{sig}/\Delta\text{sig}}$  mice ( $n=9$  for each genotype). (E-G) Mice cremaster muscle arterioles were subjected to the laser-induced thrombosis model as described in the *Online Supplementary Appendix*. Curves represent median integrated fluorescence intensity (IFI) from platelets (arbitrary units: AU) (E) or fibrinogen (F) as a function of time after the injury (20 thrombi in 3  $Gplb\alpha^{+/+}$  and 34 thrombi in 4  $Gplb\alpha^{\Delta\text{sig}/\Delta\text{sig}}$  mice). (G) Representative composite fluorescence images of platelets (green) and fibrin (red) with bright field images after laser-induced injury of the endothelium of  $Gplb\alpha^{+/+}$  (top panels) vs.  $Gplb\alpha^{\Delta\text{sig}/\Delta\text{sig}}$  mice (bottom panels). Scale bar represents  $10\ \mu\text{m}$ . Each symbol represents one thrombus. Horizontal lines intersecting the data set represent the median. Data was analyzed using Mann Whitney test; ns:  $P>0.05$ . Also see the *Online Supplementary Video S1* and the *Online Supplementary Figure S1*. FSC: forward scatter; Hb: hemoglobin.

and G; *Online Supplementary Figure S2C to D*).<sup>9,19</sup> When experiments were performed in the presence of both botrocetin and GR144053, which competitively inhibits the interaction of  $\alpha$ IIb $\beta$ 3 with VWF and/or fibrinogen, the number of *GPIb $\alpha$ <sup>+/+</sup>* platelets forming filopodia was not appreciably influenced (*Online Supplementary Figure S2B*), but the proportion of that formed >3 filopodia was significantly reduced ( $37\pm 6.7\%$  vs.  $74\pm 6.9\%$ ) (*Online Supplementary Figure S2A*), revealing the contribution of outside-in signaling to filopodia formation. Under these conditions, here again although *GPIb $\alpha$ <sup>Asig/Asig</sup>* platelets bound VWF surfaces, they had a significantly diminished ability to form filopodia (Figure 3E and H). Moreover, GR144053 had no effect upon filopodia formation in *GPIb $\alpha$ <sup>Asig/Asig</sup>* platelets (*Online Supplementary Figure S2C*), suggesting that the reduced filopodia formation in these platelets was likely

due to a defect in VWF-GPIb $\alpha$  signaling manifest by a lack of activation of  $\alpha$ IIb $\beta$ 3 in response to VWF-GPIb $\alpha$  binding. Taken together, these results indicate that deletion of the last 24 a.a. of the intracellular tail of GPIb $\alpha$  does not influence platelet binding to VWF, but significantly reduces VWF-GPIb $\alpha$  downstream signaling response including  $\alpha$ IIb $\beta$ 3 activation.

### The intracellular tail of GPIb $\alpha$ is important for GPVI signaling

We next evaluated agonist-induced platelet activation in *GPIb $\alpha$ <sup>Asig/Asig</sup>* mice. In response to ADP, washed *GPIb $\alpha$ <sup>Asig/Asig</sup>* platelets exhibited normal  $\alpha$ IIb $\beta$ 3 activation and P-selectin exposure and normal platelet aggregation (Figure 4A to D). Responses to thrombin were also normal except for a slight significant decrease in P-selectin exposure with the lowest

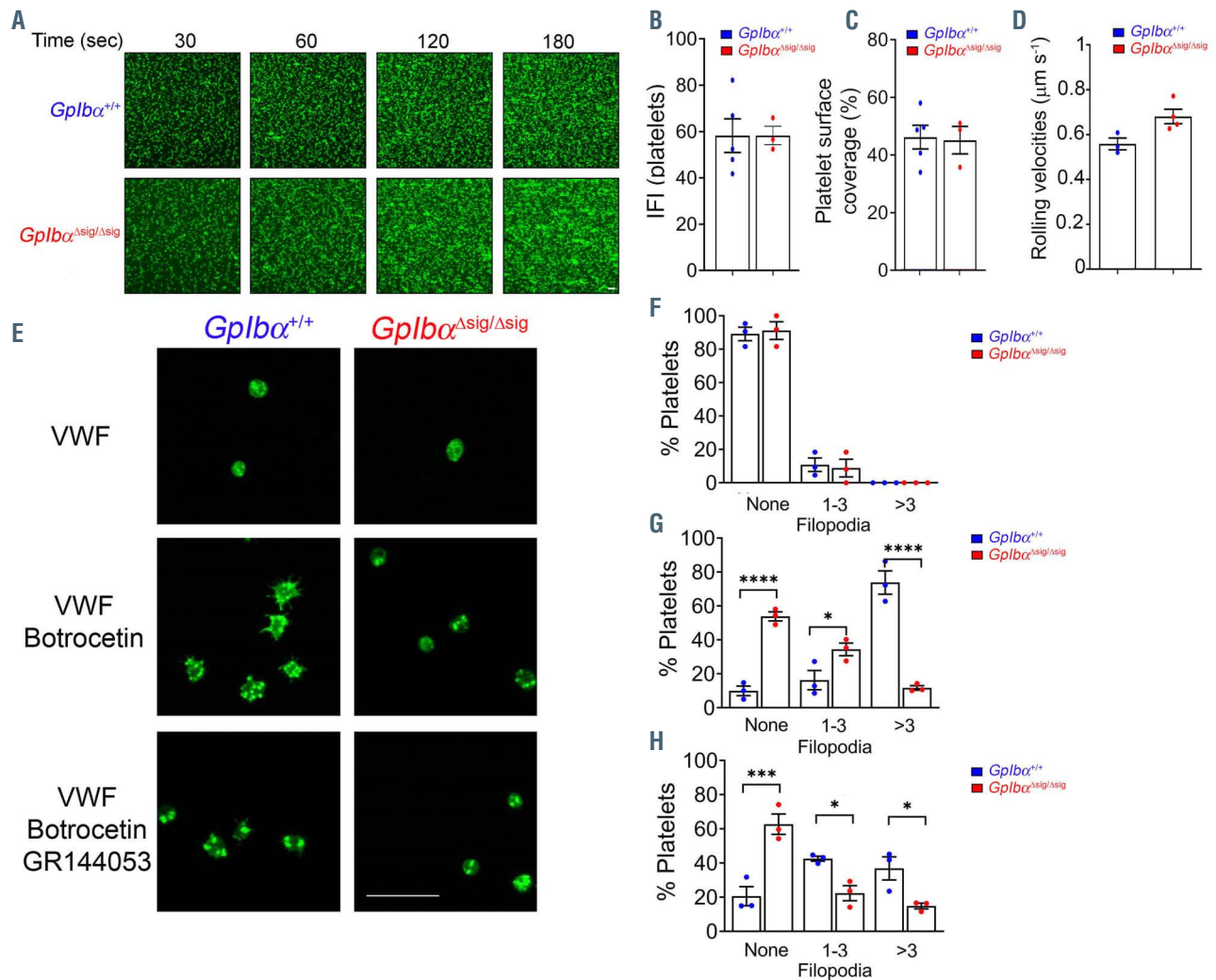


**Figure 3.** *GPIb $\alpha$ <sup>Asig/Asig</sup>* platelets exhibit normal binding to von Willebrand factor but disrupted GPIb $\alpha$ -mediated signaling. (A-D) Plasma-free blood from *GPIb $\alpha$ <sup>+/+</sup>* and *GPIb $\alpha$ <sup>Asig/Asig</sup>* mice supplemented with anti-GPIIb-DyLight488 antibody was perfused over murine VWF at a shear rate of  $1,000 \text{ s}^{-1}$ . (A) Representative fluorescence images ( $n \geq 3$ ; scale bar  $10 \mu\text{m}$ ) and bar graphs analyzing the integrated fluorescence intensity (IFI) (B) and the surface coverage (C) of *GPIb $\alpha$ <sup>+/+</sup>* and *GPIb $\alpha$ <sup>Asig/Asig</sup>* platelets captured by murine von Willebrand factor (VWF) after 3.5 minutes of flow. (D) Rolling velocities (median  $\pm$  confidence interval [CI]) were calculated from (approximately 10,000) platelets rolling/adhering to murine VWF within the first 30 seconds ( $n \geq 3$ ) (E) Representative confocal images of *GPIb $\alpha$ <sup>+/+</sup>* and *GPIb $\alpha$ <sup>Asig/Asig</sup>* platelets ( $n=3$  for each genotype) spread on mVWF and stained with Phalloidin-Alexa 488, in the absence or presence of Botrocetin or Botrocetin and GR144053 (scale bar  $10 \mu\text{m}$ ). (F to H) Percentage of platelets from *GPIb $\alpha$ <sup>+/+</sup>* and *GPIb $\alpha$ <sup>Asig/Asig</sup>* mice (individual data points representing the average of 3-6 fields of view) with no filopodia, 1-3 filopodia or >3 filopodia formed on murine VWF in the absence (F); 129 *GPIb $\alpha$ <sup>+/+</sup>* platelets and 115 *GPIb $\alpha$ <sup>Asig/Asig</sup>* platelets analysed) or presence of Botrocetin (G; 511 *GPIb $\alpha$ <sup>+/+</sup>* platelets and 547 *GPIb $\alpha$ <sup>Asig/Asig</sup>* platelets analysed), or Botrocetin and GR144053 (H; 359 *GPIb $\alpha$ <sup>+/+</sup>* platelets and 480 *GPIb $\alpha$ <sup>Asig/Asig</sup>* platelets analysed). Data represents mean  $\pm$  standard error of the mean (B, C, F to H) or median  $\pm$  CI (D) and was analyzed using unpaired two-tailed Student's *t*-test (B and C), unpaired Mann Whitney test (D) or using two-way ANOVA followed by Sidak's multiple comparison test (F to H); \* $P < 0.05$ , \*\* $P < 0.001$ , \*\*\* $P < 0.0001$ . Also see the *Online Supplementary Figure S2* and the *Online Supplementary Video S2*.

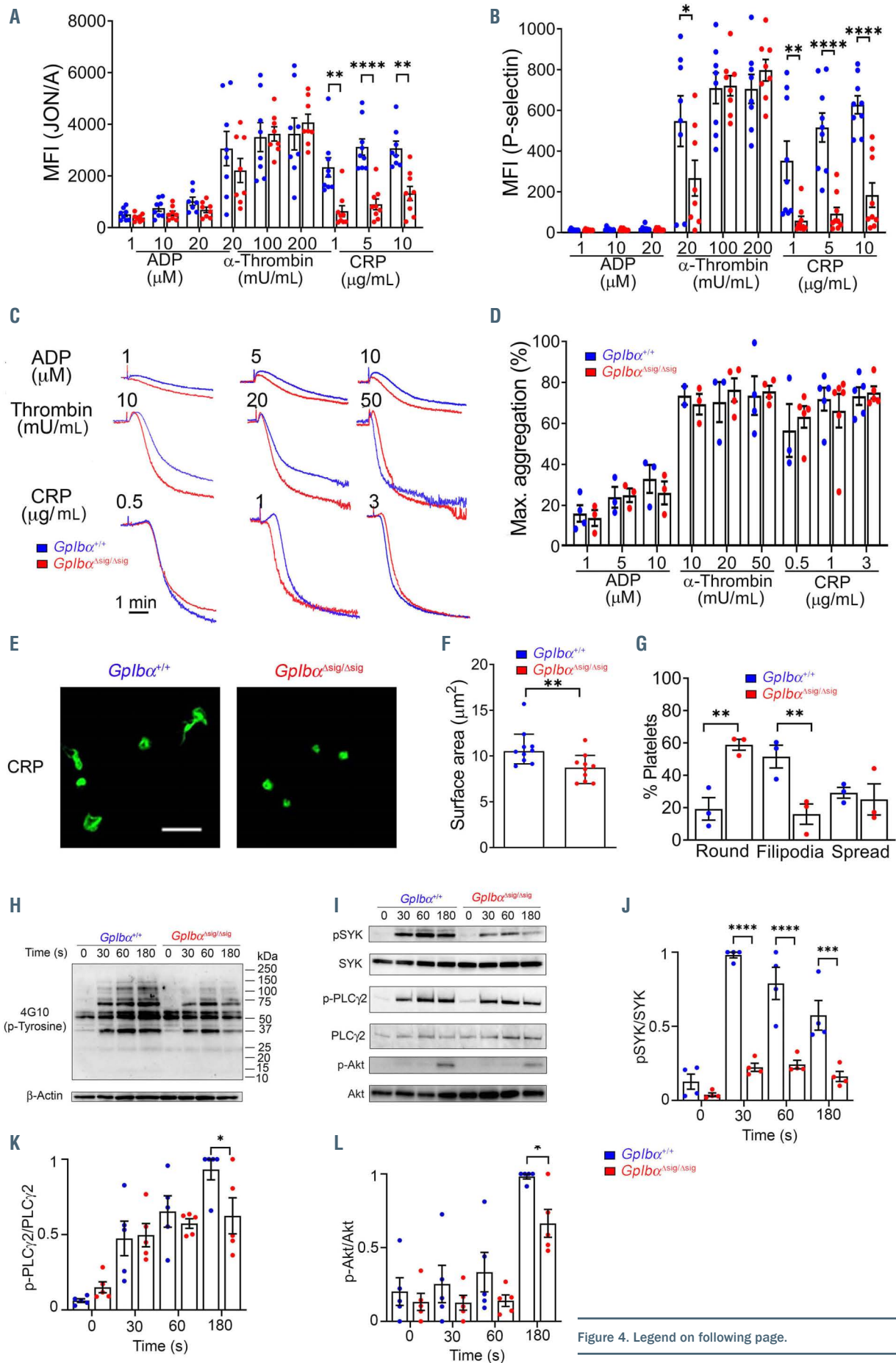


Figure 4. Legend on following page.

**Figure 4.** *Gplb $\alpha$ <sup>Asig/Asig</sup>* platelets exhibit altered GPVI-mediated signaling. (A and B) Flow cytometric analysis of surface expression of activated  $\alpha$ IIb $\beta$ 3 (A) and P-selectin (B) in *Gplb $\alpha$ <sup>+/+</sup>* and *Gplb $\alpha$ <sup>Asig/Asig</sup>* platelets (n=8) in response to ADP (1-20  $\mu$ M),  $\alpha$ -thrombin (20-200 mU/mL), or CRP (1-10  $\mu$ g/mL). MFI: geometric mean fluorescence intensity (C) Representative aggregation traces (n=3-6) of washed platelets isolated from *Gplb $\alpha$ <sup>+/+</sup>* (blue) or *Gplb $\alpha$ <sup>Asig/Asig</sup>* (red) mice and stimulated with ADP (1-10  $\mu$ M),  $\alpha$ -thrombin (20-50 mU/mL) or CRP (0.5-3  $\mu$ g/mL). Aggregation was monitored using a Chronolog aggregometer over 6 minutes. (D) Bar graph analysing the maximum aggregation (%) obtained in the conditions presented in (C). (E) Representative micrographs (n=3 for each genotype; 3 fields of view analyzed per condition; scale bar 10  $\mu$ m) of 454 *Gplb $\alpha$ <sup>+/+</sup>* and 420 *Gplb $\alpha$ <sup>Asig/Asig</sup>* platelets spread on CRP and stained with Phalloidin-Alexa 488. Bar graphs quantifying the surface area (F) and percentages (G) of platelets that remained round, formed filopodia or spread on CRP. (H) Western blot analyzing tyrosine kinase phosphorylation in platelets from *Gplb $\alpha$ <sup>+/+</sup>* and *Gplb $\alpha$ <sup>Asig/Asig</sup>* mice, following stimulation with 3  $\mu$ g/mL CRP for 0-180 seconds (s), using  $\beta$ -actin as a loading control (representative of n=3). (I) Western blots analyzing the levels of phosphorylated and non-phosphorylated SYK, PLC $\gamma$ 2 and Akt in platelets from *Gplb $\alpha$ <sup>+/+</sup>* and *Gplb $\alpha$ <sup>Asig/Asig</sup>* mice, after 0-180 s stimulation with CRP (representative of n=3). (J-L) Bar graphs displaying the levels of phosphorylated SYK, PLC $\gamma$ 2 and Akt in platelets from *Gplb $\alpha$ <sup>+/+</sup>* and *Gplb $\alpha$ <sup>Asig/Asig</sup>* mice, after 0-180 s stimulation with CRP and normalizing the intensity according to the non-phosphorylated levels of SYK, PLC $\gamma$ 2 and Akt. For the surface area (F), the data represent the median  $\pm$  confidence interval (CI) and was analyzed using the unpaired Mann Whitney test. All other data is displayed as mean  $\pm$  standard error of the mean and was analyzed using two-way ANOVA followed by Sidak's multiple comparison test. \* $P$ <0.05, \*\* $P$ <0.01, \*\*\* $P$ <0.001, \*\*\*\* $P$ <0.0001. Also see the *Online Supplementary Figures S2 and S3*.

thrombin concentration (Figure 4A and B) but this did not influence thrombin-induced platelet aggregation (Figure 4C and D). How this reduced P-selectin exposure in response to low thrombin concentration is manifest remains unclear, but may reflect the findings of a previous study that suggested the importance of 14-3-3 $\zeta$  binding to GPIIb/IIIa specifically for low-dose thrombin responses.<sup>40</sup> Despite largely unaffected responses to ADP and thrombin, in response to collagen-related peptide (CRP), *Gplb $\alpha$ <sup>Asig/Asig</sup>* platelets exhibited markedly reduced  $\alpha$ IIb $\beta$ 3 activation and P-selectin exposure (Figure 4A and B). Interestingly, *Gplb $\alpha$ <sup>Asig/Asig</sup>* platelet aggregation following CRP stimulation appeared normal (Figure 4C and D).

Next, we evaluated the ability of *Gplb $\alpha$ <sup>Asig/Asig</sup>* platelets to spread on fibrinogen surfaces with and without prior stimulation with thrombin. Without platelet stimulation, similar to wild-type platelets, most *Gplb $\alpha$ <sup>Asig/Asig</sup>* platelets remained round while upon stimulation with thrombin approximately 80% platelets spread fully with no difference observed in the spread platelet area (*Online Supplementary Figure S3A to E*). As full spreading is highly dependent upon outside-in signaling through  $\alpha$ IIb $\beta$ 3,<sup>41</sup> this suggests that this signaling pathway is unaffected in *Gplb $\alpha$ <sup>Asig/Asig</sup>* platelets. We then explored the ability of platelets to spread on CRP-coated surfaces. Consistent with diminished platelet activation in response to CRP, *Gplb $\alpha$ <sup>Asig/Asig</sup>* platelets remained round in contrast to wild-type platelets (59 $\pm$ 3.4% vs. 19 $\pm$ 7%; Figure 4E and G). This effect was also quantified by a 20% reduction in bound platelet area (Figure 4F) and in the reduced incidence of filopodia formation – 16 $\pm$ 6.3% for *Gplb $\alpha$ <sup>Asig/Asig</sup>* versus 52 $\pm$ 7.1% for *Gplb $\alpha$ <sup>+/+</sup>* (Figure 4E and G). Collectively, these results reveal an appreciable defect in GPVI-mediated signaling in *Gplb $\alpha$ <sup>Asig/Asig</sup>* platelets.

There was an overall reduction in tyrosine phosphorylation after CRP stimulation in *Gplb $\alpha$ <sup>Asig/Asig</sup>* platelets compared to wild-type platelets (Figure 4H). Further analysis revealed appreciably reduced Syk kinase activation in *Gplb $\alpha$ <sup>Asig/Asig</sup>* platelets, as measured by phosphorylation of Syk on Tyr525 and Tyr526 in response to CRP and lower phosphorylation levels of its downstream target pPLC $\gamma$ 2 (p-Tyr 1217), although this was less marked than for those observed with pSyk (Figure 4I to K). In addition, phosphorylation levels of Akt (p-Ser 473), a known substrate of PI3K were also appreciably diminished in *Gplb $\alpha$ <sup>Asig/Asig</sup>* versus *Gplb $\alpha$ <sup>+/+</sup>* (Figure 4I and L). In order to assess whether the effect of truncation of GPIIb/IIIa was specific for GPVI-mediated platelet responses, or whether other tyrosine-mediated signaling pathways might also be affected, we stimulated *Gplb $\alpha$ <sup>Asig/Asig</sup>* and wild-type platelets with rhodocytin (C-type lectin receptor 2 [CLEC-2] agonist). Tyrosine-phosphorylation profile of *Gplb $\alpha$ <sup>Asig/Asig</sup>* platelets in response to rhodocytin was similar to that of *Gplb $\alpha$ <sup>+/+</sup>* platelets, with slightly

reduced phosphorylation of Syk (approximately 20%) (*Online Supplementary Figure S4A to C*). P-selectin exposure in response to rhodocytin was reduced in *Gplb $\alpha$ <sup>Asig/Asig</sup>* platelets while  $\alpha$ IIb $\beta$ 3 activation was only diminished for the lowest concentration of the toxin without reaching statistical significance (*Online Supplementary Figure S4D to E*). These results suggest that the GPIIb/IIIa tail may also influence CLEC-2 ITAM-mediated signaling, but perhaps with reduced dependency.

### The role of the GPIIb/IIIa intracellular tail in platelet recruitment and aggregation under flow

In order to examine the consequences of the combined effects of disrupted VWF-GPIIb/IIIa signaling and diminished GPVI signaling in platelets in more physiological assays, we quantified platelet recruitment and aggregate formation on collagen-coated microchannels under flow. Experiments were performed at high (3,000 s<sup>-1</sup>), medium (1,000 s<sup>-1</sup>) and low (200 s<sup>-1</sup>) shear, as platelet recruitment is increasingly dependent on VWF-GPIIb/IIIa as shear increases while subsequent platelet aggregate formation on collagen surfaces becomes more dependent upon GPVI signaling.<sup>42-44</sup>

Perfusing whole blood at 3,000 s<sup>-1</sup> and 1,000 s<sup>-1</sup> over collagen, we observed a marked reduction in surface coverage of *Gplb $\alpha$ <sup>Asig/Asig</sup>* platelets when compared to *Gplb $\alpha$ <sup>+/+</sup>* platelets (Figure 5A and B; Figure 6A and B; *Online Supplementary Videos S3 and S4*). *Gplb $\alpha$ <sup>Asig/Asig</sup>* platelets that bound to collagen also formed smaller aggregates than *Gplb $\alpha$ <sup>+/+</sup>* platelets (Figures 5C and 6C), likely reflecting the subsequent effect of diminished collagen-GPVI signaling. Perfusing wild-type plasma-free blood (to remove soluble VWF and fibrinogen) in collagen-coated microchannels revealed a significant reduction of both platelet adhesion and thrombus growth to similar levels observed in *Gplb $\alpha$ <sup>Asig/Asig</sup>* samples (Figure 6A, B, D and E) showing that a small amount of VWF-independent binding to collagen occurs at 1,000 s<sup>-1</sup>. When whole blood experiments were performed in the presence of GR144053, to block  $\alpha$ IIb $\beta$ 3, *Gplb $\alpha$ <sup>+/+</sup>* platelets were recruited to the collagen surface as a monolayer. However, additional platelet-platelet recruitment was abolished and therefore there was limited thrombus growth in 3D. This was measured by an increase in surface coverage with a decrease in thrombus formation (i.e., total platelet fluorescence; Figure 6A, B and D).<sup>45</sup> Surface coverage as well as platelet accumulation of *Gplb $\alpha$ <sup>Asig/Asig</sup>* platelets was similar in both the absence and presence of GR144053 (Figure 6A, B and E), suggesting that lack of active  $\alpha$ IIb $\beta$ 3 is part of the platelet phenotype. In order to more specifically examine the role of GPVI in this system, we performed experiments in the presence of JAQ1, an anti-murine GPVI blocking antibody. Blocking GPVI significantly reduced surface coverage and platelet accumulation in *Gplb $\alpha$ <sup>Asig/Asig</sup>* and *Gplb $\alpha$ <sup>+/+</sup>*

platelets, revealing the important contribution of GPVI signaling at 1,000 s<sup>-1</sup> (Figure 6F to I), in stabilizing platelet recruitment and their subsequent aggregation.

At venous shear rates (200 s<sup>-1</sup>) where the dependencies on VWF and collagen are slightly different to 1,000 s<sup>-1</sup>, surface coverage of *Gplbα<sup>Asig/Asig</sup>* platelets was slightly reduced compared to *GPIbα<sup>+/+</sup>* platelets although it did not reach significance. However, thrombus growth was significantly diminished (Figure 7A to C; *Online Supplementary Video S5*). Using plasma-free blood, the surface coverage was similar for *Gplbα<sup>Asig/Asig</sup>* and *GPIbα<sup>+/+</sup>* platelets, mediated by direct (VWF-independent) interaction with collagen (Figure 7A and B). Similar to high-shear conditions, platelet accumulation under plasma-free conditions of *GPIbα<sup>+/+</sup>* platelets was significantly reduced compared to whole blood (Figure 7D) similar to those observed with *Gplbα<sup>Asig/Asig</sup>* platelets (Figure 7E). In the presence of GR144053, we saw the same increase in surface coverage of *GPIbα<sup>+/+</sup>* platelets with reduced localized 3D-platelet thrombi (Figure 7A and B) although the platelet accumulation was not significantly different to *GPIbα<sup>+/+</sup>* whole blood (Figure 7D) likely due to the increased platelet coverage. Consistent with the results obtained under high-shear conditions, the effect of increased surface coverage in the presence of GR144053 was not observed with *Gplbα<sup>Asig/Asig</sup>* platelets, nor was platelet accumulation appreciably further diminished (Figure 7A, B and E). Finally, similar to results obtained under arterial shear conditions, blocking GPVI significantly reduced surface coverage and platelet accumulation in both *Gplbα<sup>Asig/Asig</sup>* and *GPIbα<sup>+/+</sup>* platelets (Figure 7F to I). As removal of either VWF or blocking of GPVI had very similar effects, this suggests that VWF-GPIbα and GPVI-collagen binding may act synergistically to recruit platelets at low shear.

## Discussion

The ability of platelet GPIbα binding to VWF to transduce intraplatelet signaling is well-known, but the hemostatic role of the platelet ‘priming’ that follows has frequently been perceived as redundant due to the comparatively mild phenotypic changes in platelets that ensue when compared to other platelet agonists (e.g., thrombin, collagen). Using a novel *Gplbα<sup>Asig/Asig</sup>* mouse, we now demonstrate that the intracellular tail of GPIbα is important not only for transduction of VWF-GPIbα signaling, but also collagen-GPVI-mediated responses in platelets (Figure 8).

The binding of GPIbα to VWF, and of GPVI to collagen, are critical events for platelet plug formation.<sup>42,46,47</sup> Previous studies reported associations between GPIbα and GPVI, or its co-receptor Fcγ<sub>2</sub> suggesting potential interplay between these signaling pathways.<sup>25,26,28</sup> Functional crosstalk between these signaling pathways is supported by the diminished VWF-GPIbα-dependent responses in platelets deficient in GPVI and by the ability of VWF to further potentiate platelet secretion in response to CRI.<sup>13,27,28</sup>

In order to explore GPIbα signaling function and its influence upon GPVI signaling, we generated *Gplbα<sup>Asig/Asig</sup>* mice by introduction of a stop codon downstream of the main filamin binding site (a.a. 668-681), but upstream of the 14-3-3 isoforms and PI3K binding regions that are important for VWF-GPIbα signaling.<sup>8-12,48</sup> (Figure 1) This resulted in uniform production of platelets that express

GPIbα with truncated intracellular tail. This circumvented the limitations associated with studying/expressing platelet receptor complexes in heterologous cellular systems. Previously generated full knockout (*GPIbα<sup>-/-</sup>*) and also GPIbα/IL4Rα-tg mice that lack the extracellular region of GPIbα do not enable analysis of VWF signaling *per se*, as they lack the ability to bind VWF, meaning that one cannot dissociate the effects of loss of VWF binding and/or VWF signaling upon functional effects upon the platelets.<sup>32,35</sup> Transgenic mice (hTg<sup>Y605X</sup>) that express human GPIbα that lacks the terminal 6 a.a. of the intracellular tail displayed reduced megakaryocyte recovery following induced thrombocytopenia,<sup>49</sup> but more recent *in vitro* studies have revealed that these mice do not lack the entire 14-3-3/PI3K binding region,<sup>9,10,12</sup> suggesting that their VWF signaling function may not be fully disrupted making interpretation of the mouse phenotype difficult.

*Gplbα<sup>Asig/Asig</sup>* mice had a modest reduction in platelet counts compared to *GPIbα<sup>+/+</sup>* littermates that is likely be attributable to the small increase in platelet size (Figure 2A and B). Interestingly, platelet size is also moderately increased in the GPIbα/IL4Rα-tg mice,<sup>35</sup> but, again, this is modest compared to the size observed in *GPIbα<sup>-/-</sup>* or in Bernard-Soulier platelets.<sup>32,33</sup> Although the major filamin binding site remains intact in *Gplbα<sup>Asig/Asig</sup>* mice, our findings may be consistent with CHO cell studies that suggested the presence of additional or extended filamin binding regions within the intracellular tail of GPIbα.<sup>48</sup> By themselves, the 20% reduction in platelet count and slight increase in platelet size would not impart a hemostatic defect.<sup>50</sup>

*Gplbα<sup>Asig/Asig</sup>* mice exhibited normal hemostatic responses to tail transection, and normal thrombus formation following mild laser-induced thrombosis (Figure 2D to G). We used a non-perforating endothelial cell injury that does not induce collagen exposure. Therefore, this non-ablative model is independent of collagen-mediated signaling pathways.<sup>36,38</sup> However, both the tail transection and laser-induced models are sensitive to VWF function.<sup>34,37</sup> Our results reveal the normal VWF-binding function of *Gplbα<sup>Asig/Asig</sup>* platelets. Normal bleeding times were also reported in hTg<sup>Y605X</sup> transgenic mice with no overt effect on platelet or coagulation functions.<sup>49</sup>

Truncation of the intracellular tail of GPIbα did not alter expression of its extracellular domain (nor influence surface expression of GPIbα, GPVI or αIIbβ3) (Figure 2C). Consequently, *Gplbα<sup>Asig/Asig</sup>* platelet capture to mouse VWF-coated surfaces was unaffected as well their rolling velocities (Figure 3A to D). Despite normal VWF binding, deletion of the PI3K and 14-3-3 binding region in GPIbα<sup>9,10,12</sup> significantly decreased filopodia extension upon stimulation of VWF binding with botrocetin but also in the presence of an αIIbβ3 antagonist that prevent outside-in signaling induced by the VWF C4 domain binding to activated αIIbβ3 (Figure 3E, G to H). Normal VWF-platelet binding in *Gplbα<sup>Asig/Asig</sup>* mice is in line with previous studies showing that deletion of the 14-3-3ζ binding site in human GPIbα in GPIb-IX CHO cells does not influence VWF binding, but does reduce their ability to spread.<sup>9,51</sup> Other studies showed that a membrane-permeable inhibitor of the 14-3-3ζ-GPIbα interaction (MP-αC) inhibited GPIbα-dependent platelet agglutination and was protective in murine thrombosis models.<sup>11,52</sup> However, although this peptide disrupts the interaction between 14-3-3ζ and GPIbα, it may also influence 14-3-3ζ function



independent of GPIIb/IIIa binding. This contention is perhaps supported by a recent study revealing that 14-3-3 $\zeta$  deficient mice are protected against arterial thrombosis with normal VWF-GPIIb/IIIa-mediated platelet function.<sup>53</sup>

In addition to defective VWF-mediated signaling, *Gplb1*<sup>Asig/Asig</sup> platelets exhibited markedly diminished collagen-mediated signaling through GPVI evidenced by reduced surface expression of P-selectin and activation of  $\alpha$ IIb $\beta$ 3, fewer filopodia upon CRP stimulation (Figure 4A, B, E to G), and severely diminished platelet aggregate formation on collagen under venous and arterial shears (Figures 5 to 7). Bernard-Soulier patient platelets have historically been reported to respond normally to collagen in aggregation assays.<sup>54</sup> However, the thrombocytopenia and giant platelets associated with full GPIIb/IIIa deficiency combined with the loss of VWF-dependent platelet recruitment on collagen impair full analysis of other platelet signaling pathways under physiological flow conditions. Interestingly, although early studies on Bernard-Soulier patients reported that platelet aggregation in response to collagen was normal, their transformation into procoagulant platelets was specifically impaired in response to collagen (but not other agonists).<sup>55</sup> More recently, a Bernard-Soulier patient with mutations in both GPIIb/IIIa and filamin A was also reported to exhibit defects in GPVI-mediated signaling responses.<sup>56</sup> Although the authors contended that this defect might be due to the filamin A mutation, this may warrant some reappraisal in light of the data presented herein. Like Bernard-Soulier platelets, we found that *Gplb1*<sup>Asig/Asig</sup> platelets aggregated normally in response to CRP (Figure 4C to D). The signaling deficit presumably allows sufficient activation of  $\alpha$ IIb $\beta$ 3 for the platelets to aggregate. This is perhaps unsurprising given that *Gp6*<sup>-/-</sup> platelet aggregation is only affected at low collagen con-

centrations.<sup>57,58</sup> Taken together, previous studies support the contention that Bernard-Soulier patient platelets exhibit a partial deficit in GPVI signaling that resembles the deficit in *Gplb1*<sup>Asig/Asig</sup> mouse platelets.

Platelets can interact with collagen directly through GPVI and  $\alpha$ 2 $\beta$ 1, and indirectly via GPIIb/IIIa binding to VWF, the latter being increasingly important as shear rates rise to first capture the platelets and enable the aforementioned direct interactions to take place.<sup>42,59</sup> This is demonstrated in wild-type mice, similar to previous reports,<sup>43,60</sup> by the markedly reduced binding of platelets to collagen in the absence of plasma (and therefore VWF) at medium shear rates (Figure 6A, B and D). Although we demonstrated that *Gplb1*<sup>Asig/Asig</sup> platelets bind VWF normally, we saw the largest defect in platelet coverage/accumulation when compared to wild-type mice at 3,000 s<sup>-1</sup> (Figure 5). Based on these results, it seems likely that VWF-GPIIb/IIIa signaling is also important at these high shear rates, similar to the importance of GPIIb/IIIa binding to VWF for platelet tethering. We therefore contend that under medium/high shear conditions, VWF-GPIIb/IIIa platelet priming induces some rapid activation of  $\alpha$ IIb $\beta$ 3, which enable the platelets to better withstand the higher shear rates, prior to their interaction/activation by collagen (Figure 8). Although most evident at the highest shear rates, *Gplb1*<sup>Asig/Asig</sup> platelets exhibited reduced accumulation at venous shear rates (Figure 7C). Given that the surface coverage on collagen was not significantly altered at 200 s<sup>-1</sup> in *Gplb1*<sup>Asig/Asig</sup> platelets compared to wild-type platelets (Figure 7A and B), the deficit in subsequent platelet accumulation must be due to reduced reactivity of *Gplb1*<sup>Asig/Asig</sup> platelets. This is supported by the clear importance of  $\alpha$ IIb $\beta$ 3 activation to this assay, demonstrated by the effects of GR144053 in preventing 3D accumulation of platelets at both 200 s<sup>-1</sup> and 1,000 s<sup>-1</sup> in wild-

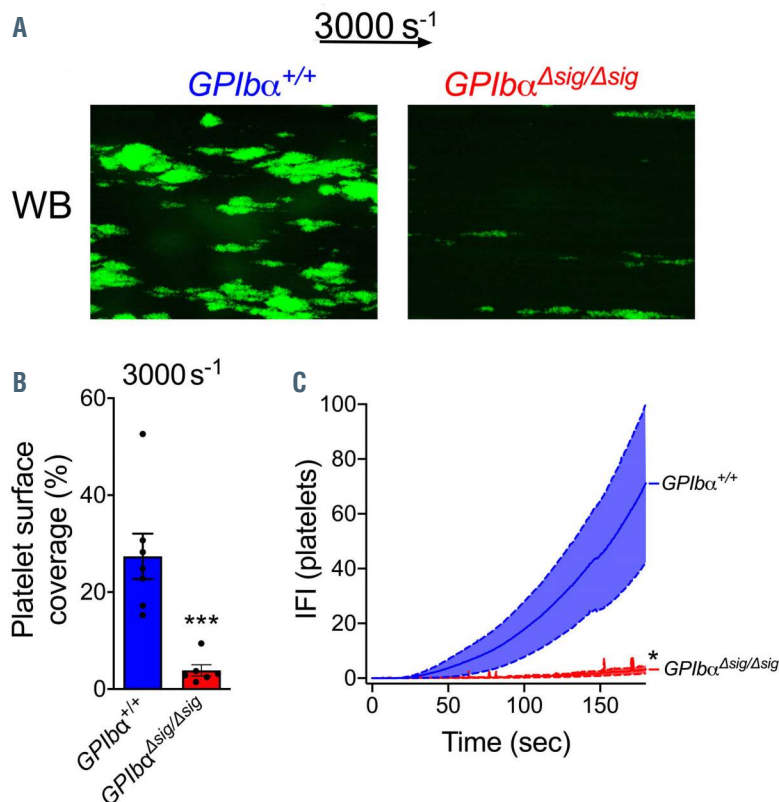


**Figure 5.** *Gplb1*<sup>Asig/Asig</sup> platelets have a reduced ability to bind to collagen and form microthrombi at 3,000 s<sup>-1</sup>. Hirudin anticoagulated whole blood from *Gplb1*<sup>+/+</sup> and *Gplb1*<sup>Asig/Asig</sup> mice was labeled with anti-GPIIb/IIIa-DyLight488 antibody and perfused over fibrillar collagen type I (0.2 mg/mL) at a shear rate of 3,000 s<sup>-1</sup> for 3 minutes. (A) Representative fluorescence images (n=6) after 3 minutes of perfusion in whole blood (WB) from *Gplb1*<sup>+/+</sup> and *Gplb1*<sup>Asig/Asig</sup> mice at 3,000 s<sup>-1</sup>. Platelet deposition (B) and thrombus build-up measured as integrated fluorescence intensity (IFI) (C). All data is shown as mean  $\pm$  standard error of the mean and analyzed using unpaired two-tailed student's t-test. The maximal platelet IFI was used to compare the thrombus build up data. \* $P < 0.05$ , \*\*\* $P < 0.001$ . Scale bar 100  $\mu$ m. Also see the *Online Supplementary Video S3*.

type platelets (Figure 6A to D; Figure 7A to D). We also observed an increase in the platelet coverage in wild-type platelets in the presence of the  $\alpha$ IIb $\beta$ 3 blocker. This is in line with our previous study and others showing that  $\alpha$ IIb $\beta$ 3 blockade allows the formation of a platelet monolayer, but prevents thrombus growth in 3D and also lateral platelet-platelet aggregation (Figure 6B; Figure 7B).<sup>5,45,61,62</sup> This underscores the importance in quantifying both platelet coverage and accumulation in flow assays when studying platelet signaling defects.<sup>45,61</sup> Importantly, GR144053 did not alter these parameters when added to

*Gplb $\alpha$ <sup>Asig/Asig</sup>* platelets (Figure 6A, B, D and E; Figure 7A, B, D and E), demonstrating a lack of  $\alpha$ IIb $\beta$ 3 activation that would be consistent with a diminished GPVI-mediated signaling response. It is important to note that this response is diminished, rather than ablated as the addition of JAQ1 led to a marked decrease in both platelet tethering and accumulation at both 1,000 s<sup>-1</sup> and 200 s<sup>-1</sup> shear rates (Figure 6F to I; Figure 7F to I). The question remains open as to the precise contribution of VWF-GPIb $\alpha$  versus collagen-GPVI signaling deficits to the phenotype of *Gplb $\alpha$ <sup>Asig/Asig</sup>* platelets. Our data suggest that both signaling pathways likely con-

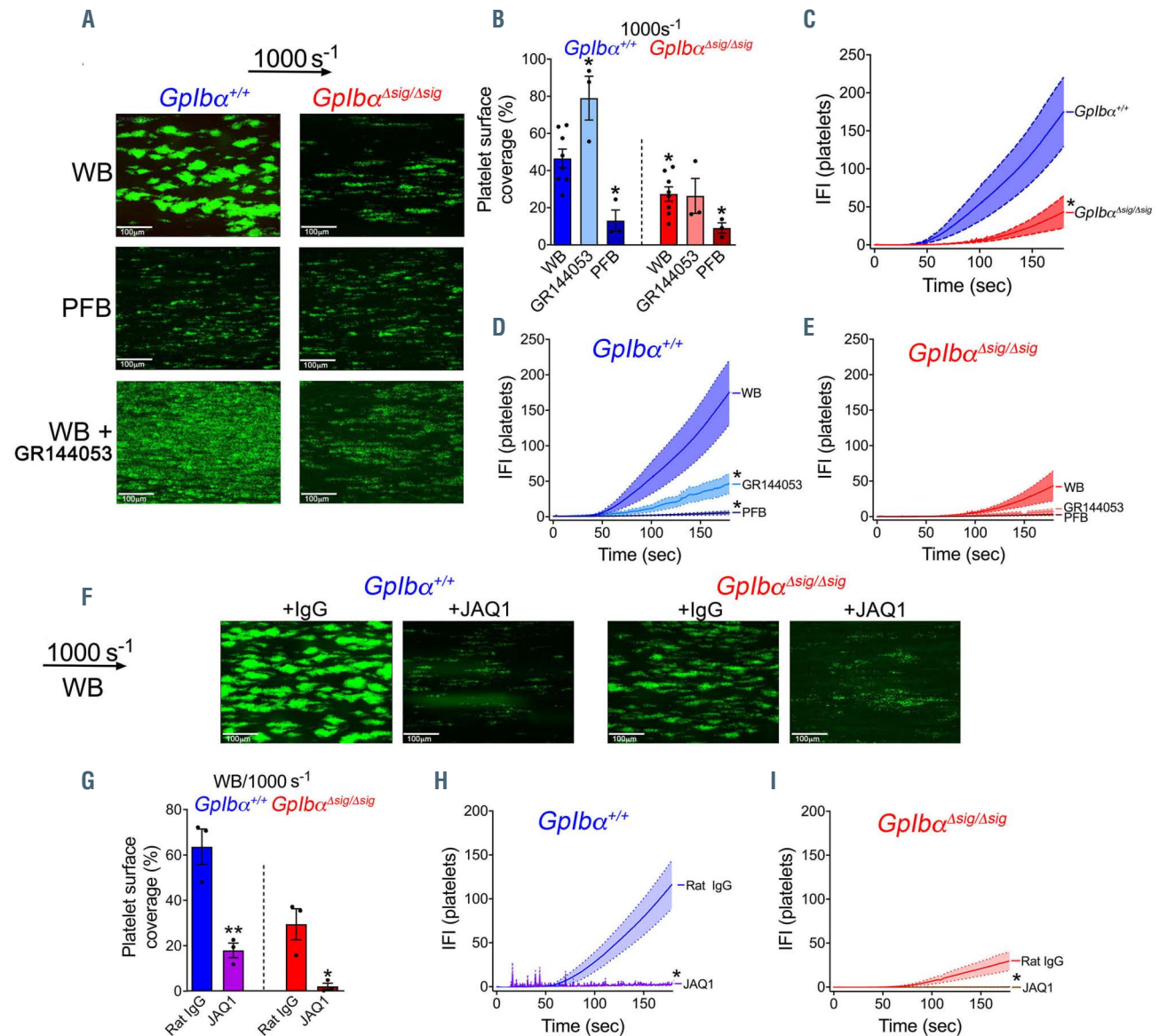


**Figure 6.** *Gplb $\alpha$ <sup>Asig/Asig</sup>* platelets have a reduced ability to bind to collagen and form microthrombi at 1,000 s<sup>-1</sup>. (A to E) Hirudin anticoagulated whole blood supplemented or not with GR144053 or plasma-free blood from *Gplb $\alpha$ <sup>+/+</sup>* and *Gplb $\alpha$ <sup>Asig/Asig</sup>* mice was labeled with anti-GPIb $\alpha$ -DyLight488 antibody (Ab) and perfused over fibrillar collagen type I (0.2 mg/mL) at a shear rate of 1,000 s<sup>-1</sup> for 3 minutes (min). (A) Representative fluorescence images (n $\geq$ 3) after 3 min of perfusion in whole blood (WB), plasma-free blood (PFB) or WB + GR144053 from *Gplb $\alpha$ <sup>+/+</sup>* and *Gplb $\alpha$ <sup>Asig/Asig</sup>* mice. Platelet deposition (B) and thrombus build-up measured as integrated fluorescence intensity (IFI) (C to E). All data is shown as mean  $\pm$  standard error of the mean and analyzed using unpaired two-tailed student's t-test (C) or one-way ANOVA followed by Dunnett's multiple comparison test (B, D to E). Data is compared to means from *Gplb $\alpha$ <sup>+/+</sup>* WB (B and D) or *Gplb $\alpha$ <sup>Asig/Asig</sup>* WB (E). The maximal platelet integrated fluorescence intensity (IFI) was used to compare the thrombus build up data. \**P*<0.05. Scale bar 100  $\mu$ m. Also see the *Online Supplementary Video S4*. (F to I) Hirudin anticoagulated whole blood from *Gplb $\alpha$ <sup>+/+</sup>* and *Gplb $\alpha$ <sup>Asig/Asig</sup>* mice supplemented with JAQ1 or Rat-IgG control Ab (20  $\mu$ g/mL) was labeled with anti-GPIb $\alpha$ -DyLight488 Ab and perfused over fibrillar collagen type I (0.2 mg/mL) at a shear rate of 1,000 s<sup>-1</sup> for 3 min. (F) Representative fluorescence images (n=3) after 3 min of perfusion. Platelet deposition (G) and thrombus build-up measured as IFI (H and I). All data is shown as mean  $\pm$  standard error of the mean and analyzed using unpaired two-tailed student's t-test. The maximal platelet IFI was used to compare the thrombus build up data. \**P*<0.05, \*\**P*<0.01. Scale bar 100  $\mu$ m.

tribute to this, as disruption of either interaction causes a major reduction in platelet accumulation in wild-type platelets under both venous and arterial shear rates.

GPVI belongs to the immunoglobulin superfamily and signals via tyrosine kinase phosphorylation pathways. In order to further investigate the defect in GPVI signaling in *Gplb $\alpha$ <sup>Asig/Asig</sup>* platelets, analysis of tyrosine phosphorylation downstream of GPVI revealed that SYK and PLC $\gamma$ 2 phosphorylation was reduced in *Gplb $\alpha$ <sup>Asig/Asig</sup>* platelets (Figure 4H to K). Interestingly, the diminished phosphorylation was more pronounced for SYK than for PLC $\gamma$ 2 perhaps highlighting the existence of LAT-independent mechanisms of PLC $\gamma$ 2 phosphorylation.<sup>63</sup> Interestingly, activation of

*Gplb $\alpha$ <sup>Asig/Asig</sup>* platelets via CLEC-2, another receptor that signals via an ITAM motif,<sup>64</sup> was also affected, but perhaps to a lesser extent than those mediated by GPVI (Online Supplementary Figure S4) suggesting that the function of the GPIb $\alpha$  intracellular tail is more important for GPVI mediated responses. Based on these findings, we hypothesize that the tail of GPIb $\alpha$  may be important for the docking of signaling molecules such as SYK, LAT and PLC $\gamma$ 2 that are downstream of GPVI and CLEC-2 on ITAM phosphorylated motif of the FcR $\gamma$  and CLEC-2 receptors and warrant further investigation. It would also be of interest to determine if the reduction in PI3K signaling in response to CRP stimulation (Figure 4I to L) is due to the lack of binding of

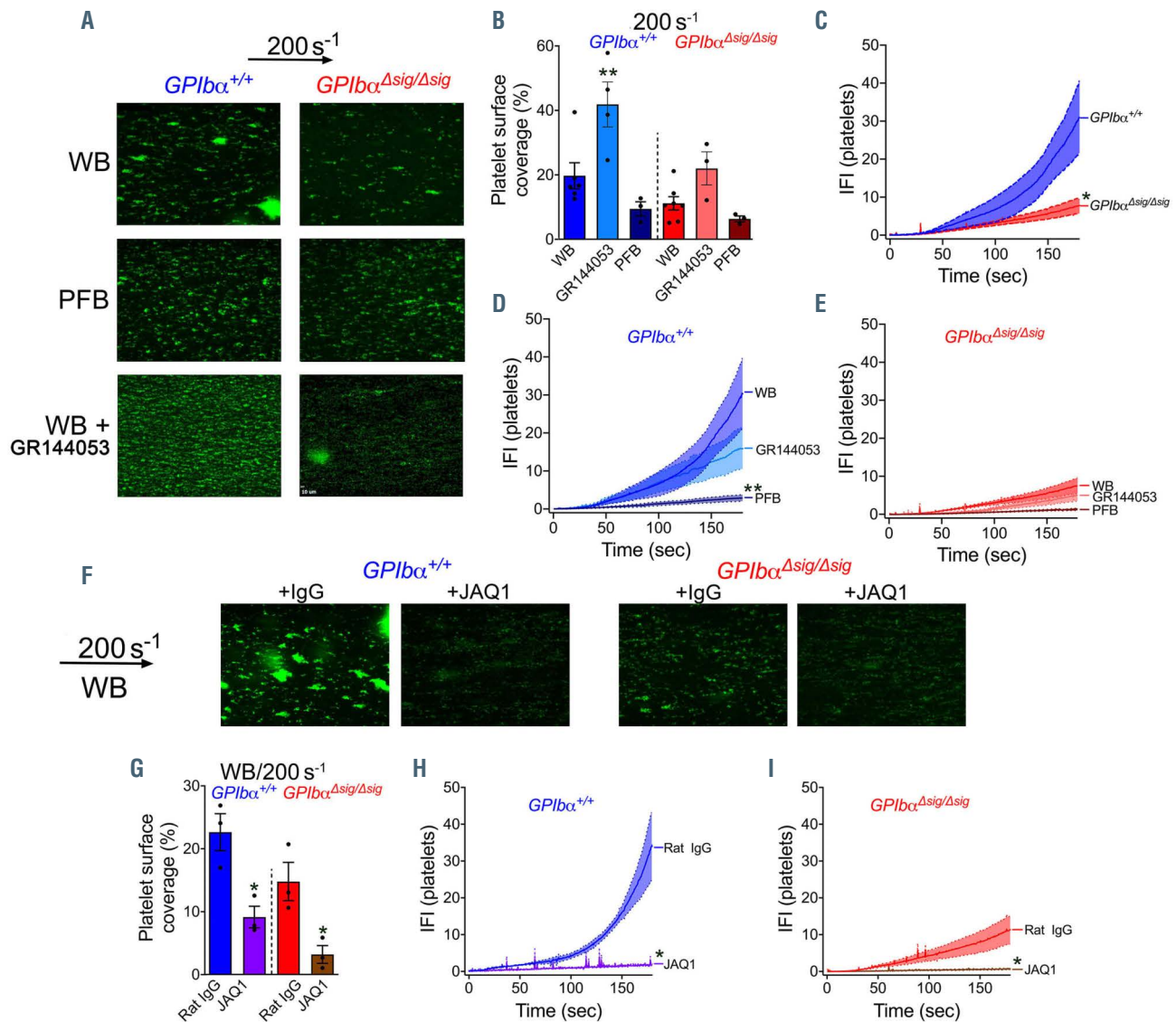


**Figure 7.** *Gplb $\alpha$ <sup>Asig/Asig</sup>* platelets have a reduced ability to bind to collagen and form microthrombi at 200 s<sup>-1</sup>. (A to E) Hirudin anticoagulated whole blood supplemented or not with GR144053 or plasma-free blood from *Gplb $\alpha$ <sup>+/+</sup>* and *Gplb $\alpha$ <sup>Asig/Asig</sup>* mice was labeled with anti-GPIb $\alpha$ -DyLight488 Ab and perfused over fibrillar collagen type I (0.2 mg/mL) at a shear rate of 200 s<sup>-1</sup> for 3 minutes (min). (A) Representative fluorescence images (n $\geq$ 3) after 3 min of perfusion in whole blood (WB), plasma-free blood (PFB) or WB + GR144053 from *Gplb $\alpha$ <sup>+/+</sup>* and *Gplb $\alpha$ <sup>Asig/Asig</sup>* mice. Platelet deposition (B) and thrombus build-up measured as integrated fluorescence intensity (IFI) (C to E). All data is shown as mean  $\pm$  standard error of the mean and analyzed using unpaired two-tailed student's *t*-test (C) or one-way ANOVA followed by Dunnett's multiple comparison test (B, D to E). Data is compared to means from *Gplb $\alpha$ <sup>+/+</sup>* WB (B and D) or *Gplb $\alpha$ <sup>Asig/Asig</sup>* WB (E). The maximal platelet integrated fluorescence intensity (IFI) was used to compare the thrombus build-up data. \**P*<0.05, \*\**P*<0.01. Scale bar 100  $\mu$ m. Also see the Online Supplementary Video S5. (F to I) Hirudin anticoagulated whole blood from *Gplb $\alpha$ <sup>+/+</sup>* and *Gplb $\alpha$ <sup>Asig/Asig</sup>* mice supplemented with JAQ1 or Rat-IgG control antibodies (20  $\mu$ g/mL) was labeled with anti-GPIb $\alpha$ -DyLight488 Ab and perfused over fibrillar collagen type I (0.2 mg/mL) at a shear rate of 200 s<sup>-1</sup> for 3 min. (F) Representative fluorescence images (n=3) after 3 min of perfusion. Platelet deposition (G) and thrombus build-up measured as IFI (H and I). All data is shown as mean  $\pm$  standard error of the mean and analyzed using unpaired two-tailed student's *t*-test. The maximal platelet IFI was used to compare the thrombus build up data. \**P*<0.05. Scale bar 10  $\mu$ m.

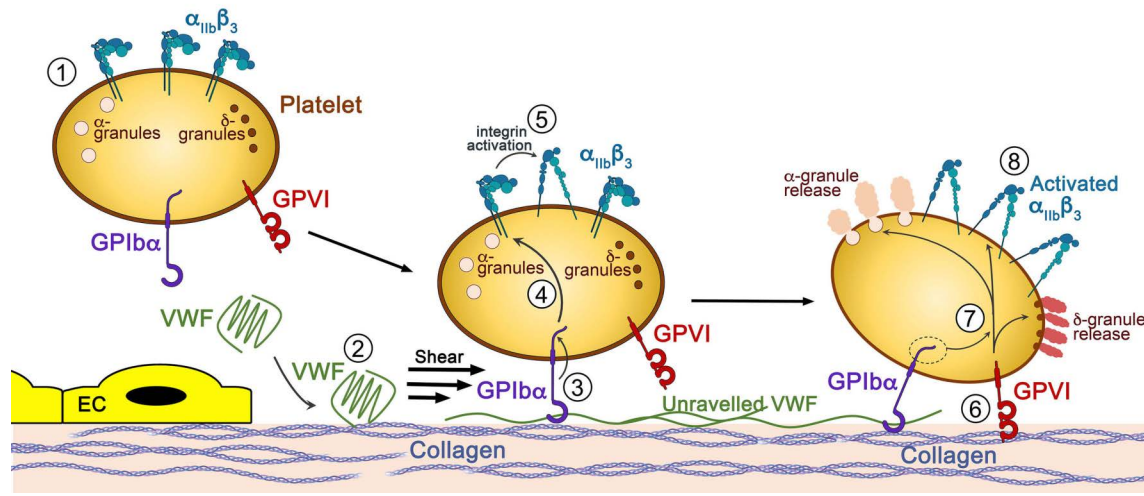


**Figure 8.** Proposed model for GPIb $\alpha$ -GPVI cross talk. Under normal conditions, resting/circulating platelets (1) present  $\alpha$ IIb $\beta$ 3 on their surface in its closed conformation. Plasma von Willebrand factor (VWF) (2) circulates in its globular conformation with its A1 domain hidden, preventing interaction with platelet GPIb $\alpha$ . Upon vascular injury, the subendothelial extracellular matrix containing collagen becomes exposed to the blood. VWF, via its A3 domain, binds to collagen and, due to shear forces, unravels to expose its A1 domain to which platelet GPIb $\alpha$  binds (3). Next, mechanosensitive signaling events downstream of VWF A1-GPIb $\alpha$  that require the intracellular tail of GPIb $\alpha$  take place leading to some activation of surface  $\alpha$ IIb $\beta$ 3 (4) while the deceleration of platelets allows for the subsequent binding of platelets to collagen via several collagen receptors including GPVI (6). The intracellular tail of GPIb $\alpha$  is also crucial for optimal collagen/GPVI signaling that lead to platelet activation, shape change and granule release (7). Ultimately, additional circulating platelets will be recruited at the site of injury to form the hemostatic plug (8).

PI3K to the intracellular tail of GPIb $\alpha$  or it is a consequence of diminished SYK phosphorylation.<sup>65</sup>

In summary, we generated a novel GPIb $\alpha$  transgenic mouse in which their platelets bind VWF normally, but the subsequent VWF-GPIb $\alpha$  signaling is disrupted. Intriguingly, these mice clearly reveal the molecular link between GPIb $\alpha$ - and GPVI-mediated signaling in platelets and underscore the cooperative functions of these two major platelet receptors.<sup>45</sup> Platelets in addition to their important role in thrombosis and hemostasis contribute to the host response to infection and inflammation.<sup>66-69</sup> Our recent work suggests that VWF-GPIb $\alpha$ -dependent platelet priming potentiates the recruitment of neutrophils, which may represent a key early event in the targeting of pathogens, but also in the development of deep vein thrombosis.<sup>5</sup> The *GPIb $\alpha$ <sup>Δsig/Δsig</sup>* mice now provide an invaluable tool to probe the importance of the GPIb $\alpha$ -mediated signaling in inflammatory diseases such as atherosclerosis and deep vein thrombosis, as well as in the host response to infection but also to fully decipher the molecular dependency of GPVI signaling upon GPIb $\alpha$ .

#### Disclosures

No conflicts of interest to disclose.

#### Contributions

AC-B designed and performed experiments, analyzed data and wrote the manuscript; YAW performed experiments and

revised the manuscript; KJW designed and performed experiments and revised the manuscript; PM and KV provided critical reagents and revised the manuscript; JTBC designed experiments, prepared the figures and wrote the manuscript; IIS-C designed and performed experiments, analyzed data, prepared the figures and wrote the manuscript.

#### Acknowledgements

The authors acknowledge the technical assistance of Alisha Müller, Elodie Ndjetehe, Ben Moyon and Zoe Webster from Central Biomedical Services and MRC transgenic group at Imperial College. We thank the LMS/NIHR Imperial Biomedical Research Center Flow Cytometry Facility for support. We would like to thank Sooriya Soman, Dr Pavarthi Sasikumar, Dr Claire Peghaire at Imperial College for technical assistance, and Nilanthi Karawitige at Imperial College Healthcare NHS trust for the use of the aggregometer. We are grateful to Professor Johannes A. Eble (University of Münster) and Dr Craig E. Hughes (University of Reading) for providing rhodocytin.

#### Funding

This work was supported by the British Heart Foundation grants FS/15/65/32036, PG/17/22/32868 and RG/18/3/33405.

#### Data sharing statement

Additional information on original data and protocols will be available upon request via email [i.salles@imperial.ac.uk](mailto:i.salles@imperial.ac.uk).

#### References

- Li R. The Glycoprotein Ib-IX-V Complex. Vol. 4th. Michelson AD, Cattaneo M, Frelinger L, Newman PJ. Platelets. Elsevier/Academic Press; 2019.
- Mazzucato M, Pradella P, Cozzi MR, De Marco L, Ruggeri ZM. Sequential cytoplasmic calcium signals in a 2-stage platelet activation process induced by the glycoprotein Ib $\alpha$  mechanoreceptor. *Blood*. 2002;100(8):2793-2800.
- Nesbitt WS, Kulkarni S, Giuliano S, et al. Distinct glycoprotein Ib/V/IX and integrin  $\alpha$ IIb $\beta$ 3-dependent calcium signals cooperatively regulate platelet adhesion under flow. *J Biol Chem*. 2002;277(4):2965-2972.
- Kasirer-Friede A, Cozzi MR, Mazzucato M, et al. Signaling through GP Ib-IX-V activates  $\alpha$ IIb $\beta$ 3 independently of other receptors. *Blood*. 2004;103(9):3403-3411.
- Constantinescu-Bercu A, Grassi L, Frontini M, et al. Activated  $\alpha$ IIb $\beta$ 3 on platelets mediates flow-dependent NETosis via SLC44A2. *Elife*. 2020;9:53353.
- Zhang W, Deng W, Zhou L, et al. Identification of a juxtamembrane mechanosensitive domain in the platelet mechanosensor glycoprotein Ib-IX complex. *Blood*. 2015;125(3):562-569.
- Ju L, Chen Y, Xue L, Du X, Zhu C.

- Cooperative unfolding of distinctive mechanoreceptor domains transduces force into signals. *Elife*. 2016;5:e15447.
8. Gu M, Xi X, Englund GD, Berndt MC, Du X. Analysis of the roles of 14-3-3 in the platelet glycoprotein Ib-IX-mediated activation of integrin  $\alpha$ (Ib) $\beta$ (3) using a reconstituted mammalian cell expression model. *J Cell Biol*. 1999;147(5):1085-1096.
  9. Mangin P, David T, Lavaud V, et al. Identification of a novel 14-3-3zeta binding site within the cytoplasmic tail of platelet glycoprotein Ibalpha. *Blood*. 2004;104(2):420-427.
  10. Mangin PH, Receveur N, Wurtz V, et al. Identification of five novel 14-3-3 isoforms interacting with the GPIb-IX complex in platelets. *J Thromb Haemost*. 2009;7(9):1550-1555.
  11. Dai K, Bodnar R, Berndt MC, Du X. A critical role for 14-3-3zeta protein in regulating the VWF binding function of platelet glycoprotein Ib-IX and its therapeutic implications. *Blood*. 2005;106(6):1975-1981.
  12. Mu FT, Andrews RK, Arthur JF, et al. A functional 14-3-3zeta-independent association of PI3-kinase with glycoprotein Ib alpha, the major ligand-binding subunit of the platelet glycoprotein Ib-IX-V complex. *Blood*. 2008;111(9):4580-4587.
  13. Wu Y, Suzuki-Inoue K, Satoh K, et al. Role of Fc receptor gamma-chain in platelet glycoprotein Ib-mediated signaling. *Blood*. 2001;97(12):3836-3845.
  14. Li Z, Zhang G, Feil R, Han J, Du X. Sequential activation of p38 and ERK pathways by cGMP-dependent protein kinase leading to activation of the platelet integrin  $\alpha$ IIb $\beta$ 3. *Blood*. 2006;107(3):965-972.
  15. Li Z, Xi X, Gu M, et al. A stimulatory role for cGMP-dependent protein kinase in platelet activation. *Cell*. 2003;112(1):77-86.
  16. Yin H, Liu J, Li Z, et al. Src family tyrosine kinase Lyn mediates VWF/GPIb-IX-induced platelet activation via the cGMP signaling pathway. *Blood*. 2008;112(4):1139-1146.
  17. Garcia A, Quinton TM, Dorsam RT, Kunapuli SP. Src family kinase-mediated and Erk-mediated thromboxane A2 generation are essential for VWF/GPIb-induced fibrinogen receptor activation in human platelets. *Blood*. 2005;106(10):3410-3414.
  18. Estevez B, Stojanovic-Terpo A, Delaney MK, et al. LIM kinase-1 selectively promotes glycoprotein Ib-IX-mediated TXA2 synthesis, platelet activation, and thrombosis. *Blood*. 2013;121(22):4586-4594.
  19. Mangin P, Yuan Y, Goncalves I, et al. Signaling role for phospholipase C gamma 2 in platelet glycoprotein Ib alpha calcium flux and cytoskeletal reorganization. Involvement of a pathway distinct from FcR gamma chain and Fc gamma RIIA. *J Biol Chem*. 2003;278(35):32880-32891.
  20. Tsuji M, Ezumi Y, Arai M, Takayama H. A novel association of Fc receptor gamma-chain with glycoprotein VI and their co-expression as a collagen receptor in human platelets. *J Biol Chem*. 1997;272(38):23528-23531.
  21. Rayes J, Watson SP, Nieswandt B. Functional significance of the platelet immune receptors GPVI and CLEC-2. *J Clin Invest*. 2019;129(1):12-23.
  22. Alshehri OM, Hughes CE, Montague S, et al. Fibrin activates GPVI in human and mouse platelets. *Blood*. 2015;126(13):1601-1608.
  23. Schmaier AA, Zou Z, Kazlauskas A, et al. Molecular priming of Lyn by GPVI enables an immune receptor to adopt a hemostatic role. *Proc Natl Acad Sci U S A*. 2009;106(50):21167-21172.
  24. Ezumi Y, Shindoh K, Tsuji M, Takayama H. Physical and functional association of the Src family kinases Fyn and Lyn with the collagen receptor glycoprotein VI-Fc receptor gamma chain complex on human platelets. *J Exp Med*. 1998;188(2):267-276.
  25. Falati S, Edmead CE, Poole AW. Glycoprotein Ib-V-IX, a receptor for von Willebrand factor, couples physically and functionally to the Fc receptor gamma-chain, Fyn, and Lyn to activate human platelets. *Blood*. 1999;94(5):1648-1656.
  26. Arthur JF, Gardiner EE, Matzaris M, et al. Glycoprotein VI is associated with GPIb-IX-V on the membrane of resting and activated platelets. *Thromb Haemost*. 2005;93(4):716-723.
  27. Goto S, Tamura N, Handa S, et al. Involvement of glycoprotein VI in platelet thrombus formation on both collagen and von Willebrand factor surfaces under flow conditions. *Circulation*. 2002;106(2):266-272.
  28. Baker J, Griggs RK, Falati S, Poole AW. GPIb potentiates GPVI-induced responses in human platelets. *Platelets*. 2004;15(4):207-214.
  29. Salles-Crawley I, Monkman JH, Ahnstrom J, Lane DA, Crawley JT. Vessel wall BAMBI contributes to hemostasis and thrombus stability [Research Support, N.I.H., Extramural Research Support, Non-U.S. Gov't]. *Blood*. 2014;123(18):2873-2881.
  30. Crawley JTB, Zalli A, Monkman JH, et al. Defective fibrin deposition and thrombus stability in Bambi(-/-) mice are mediated by elevated anticoagulant function. *J Thromb Haemost*. 2019;17(11):1935-1949.
  31. Nakamura F, Pudas R, Heikkinen O, et al. The structure of the GPIb-filamin A complex. *Blood*. 2006;107(5):1925-1932.
  32. Ware J, Russell S, Ruggeri ZM. Generation and rescue of a murine model of platelet dysfunction: the Bernard-Soulier syndrome. *Proc Natl Acad Sci U S A*. 2000;97(6):2803-2808.
  33. Lanza F. Bernard-Soulier syndrome (hemorrhagic platelet thrombocytopenic dystrophy). *Orphanet J Rare Dis*. 2006;1:46.
  34. Denis C, Methia N, Frenette PS, et al. A mouse model of severe von Willebrand disease: defects in hemostasis and thrombosis [Research Support, Non-U.S. Gov't Research Support, U.S. Gov't, P.H.S.]. *Proc Natl Acad Sci U S A*. 1998;95(16):9524-9529.
  35. Kanaji T, Russell S, Ware J. Amelioration of the macrothrombocytopenia associated with the murine Bernard-Soulier syndrome. *Blood*. 2002;100(6):2102-2107.
  36. Stalker TJ. Mouse laser injury models: variations on a theme. *Platelets*. 2020;31(4):423-431.
  37. Dubois C, Panicot-Dubois L, Gainor JF, Furie BC, Furie B. Thrombin-initiated platelet activation in vivo is vWF independent during thrombus formation in a laser injury model. *J Clin Invest*. 2007;117(4):953-960.
  38. Dubois C, Panicot-Dubois L, Merrill-Skoloff G, Furie B, Furie BC. Glycoprotein VI-dependent and -independent pathways of thrombus formation in vivo. *Blood*. 2006;107(10):3902-3906.
  39. Fukuda K, Doggett T, Laurenzi IJ, Liddington RC, Diacovo TG. The snake venom protein botrocetin acts as a biological brace to promote dysfunctional platelet aggregation. *Nat Struct Mol Biol*. 2005;12(2):152-159.
  40. Estevez B, Kim K, Delaney MK, et al. Signaling-mediated cooperativity between glycoprotein Ib-IX and protease-activated receptors in thrombin-induced platelet activation. *Blood*. 2016;127(5):626-636.
  41. Durrant TN, van den Bosch MT, Hers I. Integrin  $\alpha$ IIb $\beta$ 3 outside-in signaling. *Blood*. 2017;130(14):1607-1619.
  42. Ruggeri ZM. The role of von Willebrand factor in thrombus formation. *Thromb Res*. 2007;120 Suppl 1:S5-9.
  43. Kuijpers MJ, Schulte V, Oury C, et al. Facilitating roles of murine platelet glycoprotein Ib and  $\alpha$ IIb $\beta$ 3 in phosphatidylserine exposure during vWF-collagen-induced thrombus formation. *J Physiol*. 2004;558(Pt 2):403-415.
  44. Nieswandt B, Brakebusch C, Bergmeier W, et al. Glycoprotein VI but not  $\alpha$ 2 $\beta$ 1 integrin is essential for platelet interaction with collagen. *EMBO J*. 2001;20(9):2120-2130.
  45. Pugh N, Simpson AM, Smethurst PA, et al. Synergism between platelet collagen receptors defined using receptor-specific collagen-mimetic peptide substrata in flowing blood. *Blood*. 2010;115(24):5069-5079.
  46. Bergmeier W, Piffath CL, Goerge T, et al. The role of platelet adhesion receptor GPIbalpha far exceeds that of its main ligand, von Willebrand factor, in arterial thrombosis. *Proc Natl Acad Sci U S A*. 2006;103(45):16900-16905.
  47. Nieswandt B, Pleines I, Bender M. Platelet adhesion and activation mechanisms in arterial thrombosis and ischaemic stroke. *J Thromb Haemost*. 2011;9 Suppl 1:92-104.
  48. Feng S, Resendiz JC, Lu X, Kroll MH. Filamin A binding to the cytoplasmic tail of glycoprotein Ibalpha regulates von Willebrand factor-induced platelet activation. *Blood*. 2003;102(6):2122-2129.
  49. Kanaji T, Russell S, Cunningham J, et al. Megakaryocyte proliferation and ploidy regulated by the cytoplasmic tail of glycoprotein Ibalpha. *Blood*. 2004;104(10):3161-3168.
  50. Morowski M, Vogtle T, Kraft P, et al. Only severe thrombocytopenia results in bleeding and defective thrombus formation in mice. *Blood*. 2013;121(24):4938-4947.
  51. David T, Strassel C, Eckly A, et al. The platelet glycoprotein GPIIb/IIIa intracellular domain participates in von Willebrand factor induced-filopodia formation independently of the Ser 166 phosphorylation site. *J Thromb Haemost*. 2010;8(5):1077-1087.
  52. Yin H, Stojanovic-Terpo A, Xu W, et al. Role for platelet glycoprotein Ib-IX and effects of its inhibition in endotoxemia-induced thrombosis, thrombocytopenia, and mortality. *Arterioscler Thromb Vasc Biol*. 2013;33(11):2529-2537.
  53. Schoenwaelder SM, Darbousset R, Cranmer SL, et al. 14-3-3zeta regulates the mitochondrial respiratory reserve linked to platelet phosphatidylserine exposure and procoagulant function. *Nat Commun*. 2016;7:12862.
  54. Andrews RK, Berndt MC. Bernard-Soulier syndrome: an update. *Semin Thromb Hemost*. 2013;39(6):656-662.
  55. Walsh PN, Mills DC, Pareti FI, et al. Hereditary giant platelet syndrome. Absence of collagen-induced coagulant activity and deficiency of factor-XI binding to platelets. *Br J Haematol*. 1975;29(4):639-655.
  56. Li J, Dai K, Wang Z, et al. Platelet functional alterations in a Bernard-Soulier syndrome patient with filamin A mutation. *J Hematol Oncol*. 2015;8:79.
  57. Kato K, Kanaji T, Russell S, et al. The contri-

- bution of glycoprotein VI to stable platelet adhesion and thrombus formation illustrated by targeted gene deletion [Research Support, U.S. Gov't, P.H.S.]. *Blood*. 2003;102(5):1701-1707.
58. Mazharian A, Wang YJ, Mori J, et al. Mice lacking the ITIM-containing receptor G6b-B exhibit macrothrombocytopenia and aberrant platelet function. *Sci Signal*. 2012;5(248):ra78.
59. Nieswandt B, Watson SP. Platelet-collagen interaction: is GPVI the central receptor? *Blood*. 2003;102(2):449-461.
60. Kuijpers MJ, Schulte V, Bergmeier W, et al. Complementary roles of glycoprotein VI and alpha2beta1 integrin in collagen-induced thrombus formation in flowing whole blood *ex vivo*. *FASEB J*. 2003;17(6):685-687.
61. Pugh N, Maddox BD, Bihan D, et al. Differential integrin activity mediated by platelet collagen receptor engagement under flow conditions. *Thromb Haemost*. 2017;117(8):1588-1600.
62. Verkleij MW, Morton LF, Knight CG, et al. Simple collagen-like peptides support platelet adhesion under static but not under flow conditions: interaction via alpha2 beta1 and von Willebrand factor with specific sequences in native collagen is a requirement to resist shear forces. *Blood*. 1998;91(10):3808-3816.
63. Pasquet JM, Gross B, Quek L, et al. LAT is required for tyrosine phosphorylation of phospholipase cgamma2 and platelet activation by the collagen receptor GPVI. *Mol Cell Biol*. 1999;19(12):8326-8334.
64. Suzuki-Inoue K, Inoue O, Ozaki Y. Novel platelet activation receptor CLEC-2: from discovery to prospects. *J Thromb Haemost*. 2011;9 Suppl 1:44-55.
65. Manne BK, Badolia R, Dangelmaier C, et al. Distinct pathways regulate Syk protein activation downstream of immune tyrosine activation motif (ITAM) and hemITAM receptors in platelets. *J Biol Chem*. 2015;290(18):11557-11568.
66. Clark SR, Ma AC, Tavener SA, et al. Platelet TLR4 activates neutrophil extracellular traps to ensnare bacteria in septic blood. *Nat Med*. 2007;13(4):463-469.
67. Deppermann C, Kubes P. Platelets and infection. *Semin Immunol*. 2016;28(6):536-545.
68. Jenne CN, Kubes P. Platelets in inflammation and infection. *Platelets*. 2015;26(4):286-292.
69. Kapur R, Semple JW. Platelets as immune-sensing cells. *Blood Adv*. 2016;1(1):10-14.